REPORT DOCUMENTATION PAGE

Form Approved OMB No. 0704-0188

1. AGENCY USE ONLY (Leave blank)	2. REPORT DATE	3. REPORT TYPE AND DATES COVERED
	October 1997	Final Report

4. TITLE AND SUBTITLE

Optimal Shack-Hartmann Wavefront Sensing For Low-Light-Levels

5. FUNDING NUMBERS

F6170896W0206

6. AUTHOR(S)

Dr. Christopher J. Solomon

7. PERFORMING ORGANIZATION NAME(S) AND ADDRESS(ES)

Physics Laboratory, University of Kent at Canterbury
Canterbury CT2 7NR
United Kingdom

8. PERFORMING ORGANIZATION REPORT NUMBER

N/A

9. SPONSORING/MONITORING AGENCY NAME(S) AND ADDRESS(ES)

EOARD
PSC 802 BOX 14
FPO 09499-0200

10. SPONSORING/MONITORING AGENCY REPORT NUMBER

SPC 96-4054

11. SUPPLEMENTARY NOTES

12a. DISTRIBUTION/AVAILABILITY STATEMENT

Approved for public release; distribution is unlimited.

12b. DISTRIBUTION CODE

A

13. ABSTRACT (Maximum 200 words)

This report results from a contract tasking Physics Laboratory, University of Kent at Canterbury as follows: The contractor will investigate optimal estimation techniques for low-light-level wave-front sensing. He will analyze the sensitivity gains achievable in shach-hartmann wavefront sensors using bayesian estimators and compare the res with those achieved using a standard least squares approach. Investigate optimal wave-front sensor sub-aperture geometries.

14. SUBJECT TERMS	15. NUMBER OF PAGES
Physics	50
	16. PRICE CODE N/A

17. SECURITY CLASSIFICATION OF REPORT	18. SECURITY CLASSIFICATION OF THIS PAGE	19. SECURITY CLASSIFICATION OF ABSTRACT	20. LIMITATION OF ABSTRACT
UNCLASSIFIED	UNCLASSIFIED	UNCLASSIFIED	UL

AQ

OPTIMAL SHACK-HARTMANN WAVEFRONT SENSING FOR LOW LIGHT LEVELS

Contract F6170896 - W0206

FINAL REPORT : SPC-96-4054 - Oct 1997

C.J. Solomon
Physics Department. University of Kent. Canterbury CT2 7NR, U.K.

ABSTRACT

This report describes work carried out under contract SPC-96-4054 "Optimal Shack-Hartmann wavefront sensing for low light levels". The aim of this work has been to identify, develop and, where appropriate, implement methods for improving wavefront estimates at low light levels. The report is divided into three main sections followed by a summary and appendices. Each section addresses a major aspect of the work carried out.

- The first section considers the question of how to optimally choose the size of Hartmann subapertures for a given signal level so as to achieve the optimal wavefront estimate. After a short introduction, the main body of this section is given in the form of a paper recently submitted for publication in Optics Communications entitled "Optimal Hartmann sensing at low light levels".

- Section 2 describes the use of a Gram-Charlier matched filter to yield improved subaperture centroid estimates. The importance of the centroiding operation in wavefront sensing and adaptive optics applications is first described and the theory and results obtained with this matched filter are presented in the form of a paper recently submitted and accepted by Optics Letters - "Gram-Charlier matched filter for Shack-Hartmann sensing at low light levels".

- The third section discusses the use of both Bayesian estimators and modal projection estimation (combined with unconventional Hartmann sensor geometry) as a means to reduce noise propagation in wavefront sensing applications operating at low light level. Theory is presented together with computer simulated results for both techniques.

- The results achieved and understanding gained are given in the summary.

AQ

1. OPTIMAL SUB-APERTURE SIZE FOR HARTMANN SENSORS

When Hartmann sensors are required to operate in low signal-noise environments, there is an inherent trade-off regarding how the available signal photons should be "distributed". The Hartmann sensor is designed to provide estimates of the local slope of a wavefront averaged over a number of sample areas in the pupil plane. From these averaged slope measurements, the wavefront estimate must directly (or indirectly) be calculated. The linear estimation problem that arises has been derived and discussed in section 1 of the interim report[1]. The key point here is that whilst choice of a large number of sub-apertures (to ensure that the phase variations due to turbulence over each sub-aperture are small) will result in a small modelling error, at low light levels, this will result in a small signal in each sub-aperture and unacceptably high errors in the slope measurements. Alternatively, reducing the number of sub-apertures to a small number will reduce the noise on the slope measurements but give a larger modelling error. For a given signal-noise scenario, there will therefore be an optimum choice which minimises the overall effect on the average mean-square error of the wavefront estimate. Attempts to study this problem have been made but the analysis is somewhat idealised and crucially neglects the effect of read-noise for CCD devices which are fast becoming the de facto standard. In the following article, we present results of a study to determine optimal Hartmann sub-aperture size for different signal-noise levels. This is based on the use of a high-fidelity computer model which incorporates the effects of atmospheric turbulence, shot noise and read-noise.

OPTIMAL HARTMANN SENSING AT LOW LIGHT LEVELS

D.L. Ash, C.J. Solomon

School of Physical Sciences, University of Kent, Canterbury CT2 7NR, U.K.

G. Loos

Phillips Laboratory, Kirtland Air-Force Base, NM 87117-6008, U.S.A.

Abstract

A high-fidelity computer model has been used to investigate the performance of a Shack-Hartmann sensor operating under low light level conditions. The trade-off between sub-aperture size and slope noise is examined in detail and optimal sizes are determined for a number of imaging scenarios. Our results are discussed in relation to related literature.

1. Introduction

It is well known that atmospheric turbulence severely limits the performance of ground based telescopes and there now exists a considerable literature on both technological and computational techniques to compensate for atmospheric effects[1]. Accurate estimation of atmospherically perturbed wavefronts is of critical importance (whether directly or implicitly) in any attempt to correct incident wavefronts in real time using adaptive optics. It is also a crucial aspect of the post-processing technique of deconvolution from wavefront sensing (also termed self-referenced speckle holography) originally developed in reference[2]. Although wavefront sensing devices such as the shearing interferometer and increasingly the curvature sensor[3] have been developed and used for astronomical and surveillance imaging systems, the practical and conceptual simplicity of the Shack-Hartmann device and it's competitive performance still make it a first-choice in many systems.

In this paper, we use a high-fidelity computer model employing a modal wavefront reconstructor to investigate Hartmann sensor performance at low signal levels and consider the corresponding implications for optimal design. A key factor in employing Hartmann sensors for adaptive optics applications is to optimise the pupil-plane sub-aperture size. When the signal is limited, we see that by increasing the Hartmann sub-aperture size, the signal-noise of the individual slope measurements at the sub-apertures is increased but at the expense of larger sampling intervals and hence larger modelling error. It is evident that a balance must be achieved between these two competing factors if the best performance is to be attained.

Previous authors have addressed the question of Hartmann sub-aperture size for adaptive optics applications. Gardner et. al.[4] discuss laser-guide star adaptive optics systems and present results for that sub-aperture size which will minimise the required sub-aperture photon count to achieve a number of target rms wavefront error values. Their analysis, however, does not include the effects of read-noise. Ellerbroek[5] discusses the effect of varying $\frac{D}{l}$ (i.e. varying the number of

sub-apertures across the telescope pupil plane but this effectively only studies the fitting error. Gavel et al[6] derive analytic results for optimum sub-aperture size but under the restrictive assumption that $r_0 < 1$ and that CCD read-noise may be neglected. They also present results for the optimum sub-aperture size as a function of laser power for the Keck telescope system.

In this paper, we use a high-fidelity computer model incorporating turbulence, shot and CCD read-noise and employing a modal wavefront reconstructor to investigate Hartmann sensor performance at low signal levels. The results are discussed with regard to implications for optimal design of systems operating in low signal-noise regimes.

2. Computer Model

2.1 Generation of Hartmann images

Randomly distorted optical wavefronts obeying the Kolmogorov power spectrum were generated[7] and considered incident at the pupil plane of the telescope. As is commonly assumed in problems of imaging through turbulence, amplitude fluctuations were neglected. The Hartmann sub-aperture images were calculated by considering the appropriate segment of a high (i.e. infinite) light level wavefront and using standard Fourier optics to generate the image plane intensities as -

$$I(\xi,\eta) \propto |FT[A(x,y)]|^2 \tag{1}$$

where $I(\xi,\eta)$ is the intensity in the image plane, $A(x,y)$ is the complex amplitude of the incident wavefront portion and FT denotes the operation of Fourier transformation.

Photon limited images are generated in a standard way from the infinite light level images via generation of a cumulative distribution function which is then randomly sampled in order to determine the location of each photoelectron event in the image plane. Poisson sampling for the number of detected events in each sub-aperture is also included in the model. In our study, we have assumed a CCD camera

with read-noise of 1.5 electrons r.m.s. per pixel per frame - this figure corresponds to an upper limit on the performance of current state-of-the-art devices[8]. A number of statistical models have been described for read noise in CCD arrays[8–9]. In our study, read-noise is simulated by adding an appropriately scaled Gaussian deviate to each pixel in the CCD image frame.

Calculation of the sub-aperture centroid positions ($C(\xi,\eta) = (C_\xi, C_\eta)$) was performed using the discretised version of the classical centre of mass/first moment.

$$C_\xi = \frac{\sum_\xi \sum_\eta \xi\, I(\xi,\eta)}{\sum_\xi \sum_\eta I(\xi,\eta)}$$

$$C_\eta = \frac{\sum_\xi \sum_\eta \eta\, I(\xi,\eta)}{\sum_\xi \sum_\eta I(\xi,\eta)} \qquad (2)$$

Initially centroiding was performed over a comparatively large area to locate the approximate position of the centroid. The centroiding envelope was then reduced in size and centroiding was repeated centred on the newly estimated "spot" location. This process was then repeated iteratively until the envelope had reached the optimal dimension [10] and the centroid location had stabilised. This typically takes between 4 and 7 iterations depending on the stability tolerances specified and the rate at which the centroiding envelope is reduced.

Conversion of the centroid estimate to a local, average wavefront slope is straightforward and the slope data is then available to form an estimate of the incident wavefront.

2.2 Modal wavefront estimation

A substantial body of work has now appeared in the literature on the subject of wavefront estimation and, beginning with Wallner's paper, specifically on optimal wavefront estimation[5,13–16]. Within this body of literature, due to variations in notation and approach (i.e. integral or linear algebraic formulation), to the wavefront model (whether zonal or modal) and the specific meaning attached to optimal, the common thread amongst them is not apparent. For clarity, we here present what is,

to the best of our knowledge, the most direct and simple derivation of a maximum a posteriori (MAP) estimator for a linear model. Other common solutions used in wavefront estimation may be considered either as alternative forms or as limiting cases of this estimator.

In the so-called modal approach, the random phase function is approximated by an expansion of the form -

$$\Phi(\underline{x}) = \sum_{k=1}^{N} a_k P_k(\underline{x}) \tag{3}$$

where $\Phi(\underline{x})$ is the atmospherically distorted wavefront and $\{P_k(\underline{x})\}$ are the chosen basis functions and the system is modelled as -

$$Ax + e = m \tag{4}$$

where x is the vector of modal coefficients, A is the system or design matrix, m is the vector of phase gradients and e is the error vector on the slopes.

We make the following assumptions on this linear model (all of which are reasonable for Hartmann and shearing sensors) -

- Signal and noise vectors are both zero mean - $\langle x \rangle = \langle e \rangle = 0$.
- Noise and signal are uncorrelated $\langle x^T e \rangle = 0$.
- Noise covariance $V = \langle e e^T \rangle$ is assumed known.
- A priori covariance of the unknown vector $C_x = \langle x x^T \rangle$ is assumed known. This covariance was explicitly calculated for the Zernike basis and Kolmogorov spectrum by Noll[11]. A suitable unitary transformation enables it to be calculated for any other orthogonal basis (e.g. the Karhunen-Loeve basis)[7].

Accordingly, we seek a linear estimator $\hat{x} = Lm$ which will minimise the error covariance matrix P defined by -

$$P = \langle (x - \hat{x})(x - \hat{x})^T \rangle \tag{5}$$

We substitute $\hat{x} = L(Ax + e)$ in eq. 5 to obtain -

$$P = [I - LA] C_x [I - LA]^T + L V L^T \tag{6}$$

Taking variations in matrix P with respect to L and setting to zero[17] , we have -

$$\delta P = \delta L(AC_x[I - LA]^T + VL^T) + ([I - LA]C_x A^T + LV)\delta L^T = 0 \qquad (7)$$

which yields an optimal matrix L -

$$L_{MAP} = L = C_x A^T [AC_x A^T + V]^{-1} \qquad (7)$$

Substitution of the matrix L_{MAP} into eq. 5 defining P yields an error covariance matrix given by -

$$P_{MAP} = C_x[I - A^T[AC_x A^T + V]^{-1} AC_x] \qquad (8)$$

It is easy to show (see appendix) that two equivalent forms for L_{MAP} and P_{MAP} are -

$$\hat{x} = L_{MAP}\, m = [A^T V^{-1} A + C_x^{-1}]^{-1} A^T V^{-1} m \qquad (9)$$

$$P = P_{MAP} = [A^T V^{-1} A + C_x^{-1}]^{-1} \qquad (9)$$

Wallner's lengthy analysis reduces to this estimator under the same assumptions (see [16]) and this may also be derived directly from Bayes theorem[14-15]. Further, since since both the prior and likelihood laws on the modal coefficients may be well-modelled as gaussians[11], the choice of a different Bayesian criterion (such as finding the mean or median of the posterior distribution rather than the mode)[15] is academic and produces the same result.

In the limit that the a priori covariance tends to infinity, the MAP estimator tends to the best linear unbiassed estimator (BLUE)[18] in the mean-squared sense -

$$\hat{x} = [A^T V^{-1} A]^{-1} A^T V^{-1} m \qquad (10)$$

If we assume that the noise on each measurement is uncorrelated and the noise associated with each measurement is equal, we have $V = \sigma^2 I$ and eq. 10 gives -

$$\hat{x} = [A^T A]^{-1} A^T m \qquad (11)$$

which is recognisable as the standard least-squares solution. The standard least-squares solution is thus the limiting form of the MAP estimator when no a priori knowledge of the parameter statistics and noise is imposed or known.

Both the BLUE and MAP estimators were implemented in our computer model using the Zernike and Karhunen-Loeve bases.

3. Simulation Results

In practice, Hartmann wavefront sensing systems are limited to a finite number of sub-apertures and a finite number of modes only can be estimated. We conducted a number of studies simulating an 8 x 8 Hartmann sensor having 52 active subapertures. The primary goal was to study the variation in maximum possible compensated Strehl ratio as a function of flux and sub-aperture size. The studies were conducted using the standard least-squares modal reconstructor. As this estimator does not include a priori knowledge, no constraints are placed on the modal coefficients. It is therefore important in this case to avoid modelling errors which may be due to the use of either too few or too many modes. Accordingly, we first study modelling errors for our system. In fig. 1 we show the maximum compensated Strehl ratio as a function of the number of estimated modes with sub-aperture size fixed $= r_0$. The Strehl ratios given were generated from the residual wavefront (known wavefront subtracted from the estimated) and do not include the effects of any real phase compensating system. The incident wavefronts correspond to high light level and obey the Kolmogorov power spectrum of phase fluctuations. The wavefront reconstruction was performed using the standard least-square estimator and each data point is averaged over 400 realisations. We observe a peak at approximately 45 modes after which over-fitting effects increase the errors significantly. We also note that although the peak occurs for approximately the same number of modes, there is a significant difference between the Karhunen-Loeve basis and the Zernike polynomials.

Fig. 2 shows the effect of variations in the photoelectron flux on the optimal

value of l/r_0. Here, an 8 x 8 Hartmann sensor having 52 active subapertures was used. Read-noise was simulated at 1.5 electrons r.m.s. per pixel per frame. As intuitively expected, the peak moves towards higher values of l/r_0 as the flux falls and lower values as the flux increases. It is clear from figure 2 that the correct choice of sub-aperture size l/r_0 is of critical importance to any attempt to accurately estimate and compensate wavefronts under conditions of low incident flux. We also note that the pronounced skew in the figures indicates that choosing $\frac{l}{r_0}$ *smaller* than the optimal value has more serious consequences than slight over-estimation of the optimum value. Fig.3 shows the optimal values of l/r_0 as a function of flux levels for a number of CCD read noise values. The read-noise in fig. 3 is given in electrons per pixel per frame. In any particular imaging scenario, the temporal bandwidth required and the luminosity of the guide star will determine the frame exposure time and hence the flux. The read-noise of a CCD device for the chosen integration time can then be determined. In this way, fig. 3 may be used to directly estimate or extrapolate so as determine the optimal sub-aperture size for the given set of conditions. We point out that the Strehl ratios indicated on the graphs are *limiting values* for real adaptive optics systems which will not be achievable in practice since they entirely neglect finite bandwidth effects and limitations in the deformable mirror/correction device. However, the trend observed as l/r_0 increases is of direct relevance to real AO systems.

Since the optimal sub-aperture size clearly depends on sub-aperture signal-noise. it follows that the optimal values indicated in figure 3 are dependent on the specific centroiding algorithm and the reconstructor used. We chose to use the least-squares wavefront reconstructor because, despite the significant theoretical studies that have been made on optimal reconstructors, implementation of realistic and reliable a priori knowledge is quite complex and with notable exceptions[5] has rarely been employed in practical systems. We note that superior slope estimation based on matched filtering techniques rather than centre of mass should yield higher signal-noise at low light levels. However, since the trade-off between sub-aperture size and

slope estimation noise is such that less slope measurement noise allows smaller sub-aperture sizes, we predict that the main effect of such methods will be simply to shift the optimal sub-aperture size to slightly smaller values than those indicated. The precise amount will depend on the relative performance of the matched filter but can reasonably be expected to be small.

4. Summary

We have shown that the optimal sub-aperture size in a Hartmann sensor operating at low light levels is critically dependent on the prevailing signal to noise level and have given the optimal value for a number of situations. Critically, our results include the effect of CCD read-noise. The optimum value for a number of typical imaging scenarios may be estimated empirically from the results presented in fig.3. This may be $> 3r_0$ in very low signal-noise conditions. We note that the specific results we have obtained in fig.3 for the optimal sub-aperture size for the zero read-noise case are in good agreement with those obtained by Gardner et al (table 1 in [4]).

Acknowledgements

The authors would like to acknowledge the support provided for this work by the European Office of Aerospace Research and Development (SPC-96-4054).

References

1. See special issue "Atmospheric compensation technology". J. Opt. Soc. Am., Vol 11, No. 2, (1992)

2. J. Primot, G. Rousset and J. Fontanella, "Deconvolution from wavefront sensing: a new technique for compensating turbulence degraded images", J. Opt. Soc. Am., Vol 7, No. 9 , (1990)

3. F. Roddier, "Curvature sensing and compensation: a new concept in adap-

tive optics", Appl. Opt., Vol 27, (1988)

4. C.S. Gardner, B.M. Welsh and L.A. Thompson, "Design and performance analysis of adaptive optical telescopes using laser guide stars", Proc. I.E.E.E. Vol. 78, No. 11, (1990)

5. B.L. Ellerbroek, "First-order performance evaluation of adaptive optics systems for atmospheric turbulence compensation in extended field-of-view astronomical telescopes", J. Opt. Soc. Am., Vol 11, No. 2, (1994)

6. D.T. Gavel, J.R. Morris and R.G. Vernon, "Systematic design and analysis of laser-guide star adaptive optics systems for large telescopes", J. Opt. Soc. Am., Vol 11, No. 2, (1994)

7. N. Roddier, "Atmospheric wavefront simulation using Zernike polynomials", Opt. Eng. , Vol. 29, 1174-1180 (1990)

8. J.W. Beletic, "Use of CCD technology for fringe tracking in the CHARA array", technical report - Internal CHARA communication" (1993)

9. N. Dillon, "CCD read-noise model", technical report, Royal Observatories (1994)

10. K.A. Winick, "Cramer-Rao lower bounds on the performance of charge-coupled-device optical position estimators, J. Opt. Soc. Am. A., Vol. 3, No 11. (1986)

11. R.J. Noll, "Zernike polynomials and atmospheric turbulence", J. Opt. Soc. Am. A., Vol 66, No. 3, (1976)

12. E.P. Wallner, "Optimal wavefront correction using slope measurements", J. Opt. Soc. Am., Vol 73, 1771-1776, (1983)

13. R.J. Sasiela and J.G. Mooney, "An optical phase reconstructor based on using a multiplier-accumulator approach", S.P.I.E. Vol. 551, pp 170-174 (1985)

14. P.A. Bakut, V.E. Kirakyosants, V.A. Loginov, C.J. Solomon and J.C. Dainty, "Optimal wavefront reconstruction from a Shack-Hartmann sensor by use of a Bayesian algorithm " (Optics Communications 109 (1994)).

15. C.J. Solomon, N.J. Wooder and J.C. Dainty, " Bayesian estimation of atmospherically distorted wavefronts using Shack-Hartmann sensors ", Optical Review Vol. 2, No. 3, 1995)

16. R.G. Lane and N.F. Law, "Wavefront estimation at low light levels", Opt. Comm. , Vol.126, No.1-3, pp.19-24 (1996)

17. T.O. Lewis and P.L. Odell, "Estimation in Linear Models", (Prentice-Hall 1971).

18. G. Strang, "Introduction to applied mathematics", Wellesley Cambridge Press) ISBN 0-9614088-0-4.

FIGURE CAPTIONS

Figure 1

Fitting error: The maximum possible compensated Strehl ratio with number of basis functions. The sensor has 52 active sub-apertures of size r_0. A least-squares reconstructor was used.

Figure 2

Maximum possible compensated Strehl ratio with pupil-plane subaperture size for signal levels of 10, 15, 20, 25 and 30 photoelectrons per r_0^2. Read-noise of 2 electrons r.m.s per pixel per frame was generated.

Figure 3

Optimum subaperture size as a function of photoelectron flux for varying amounts of read-noise. Flux is in photoelectrons per r_0^2 and read-noise in electrons r.m.s per pixel per frame.

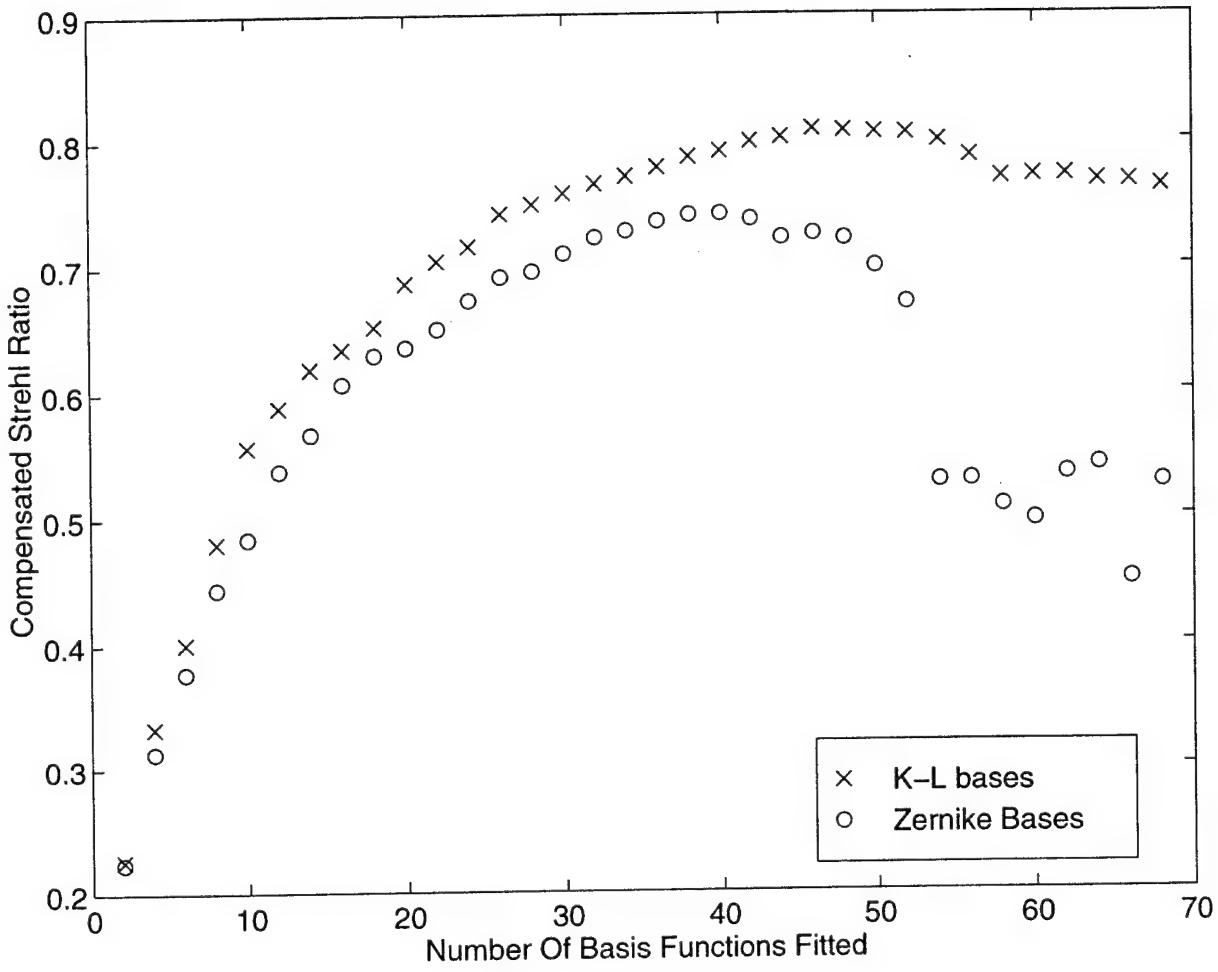
0.9
0.8
0.7
0.6
0.5
0.4
0.3
0.2
Compensated Strehl Ratio
0
10
20
30
40
50
60
70
Number Of Basis Functions Fitted
K–L bases
Zernike Bases

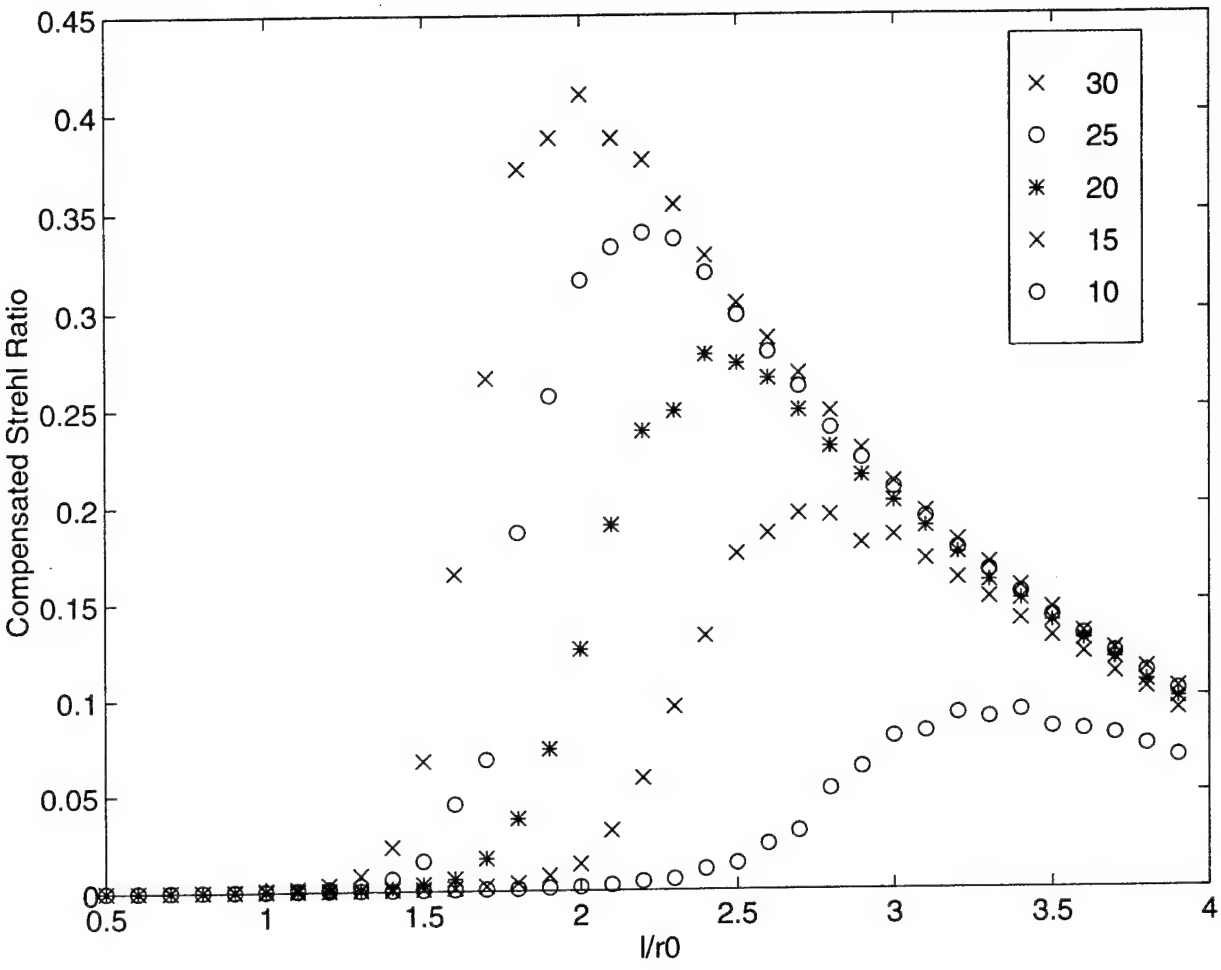
Compensated Strehl Ratio
l/r0
0.45
0.4
0.35
0.3
0.25
0.2
0.15
0.1
0.05
0
0.5
1
1.5
2
2.5
3
3.5
4
30
25
20
15
10

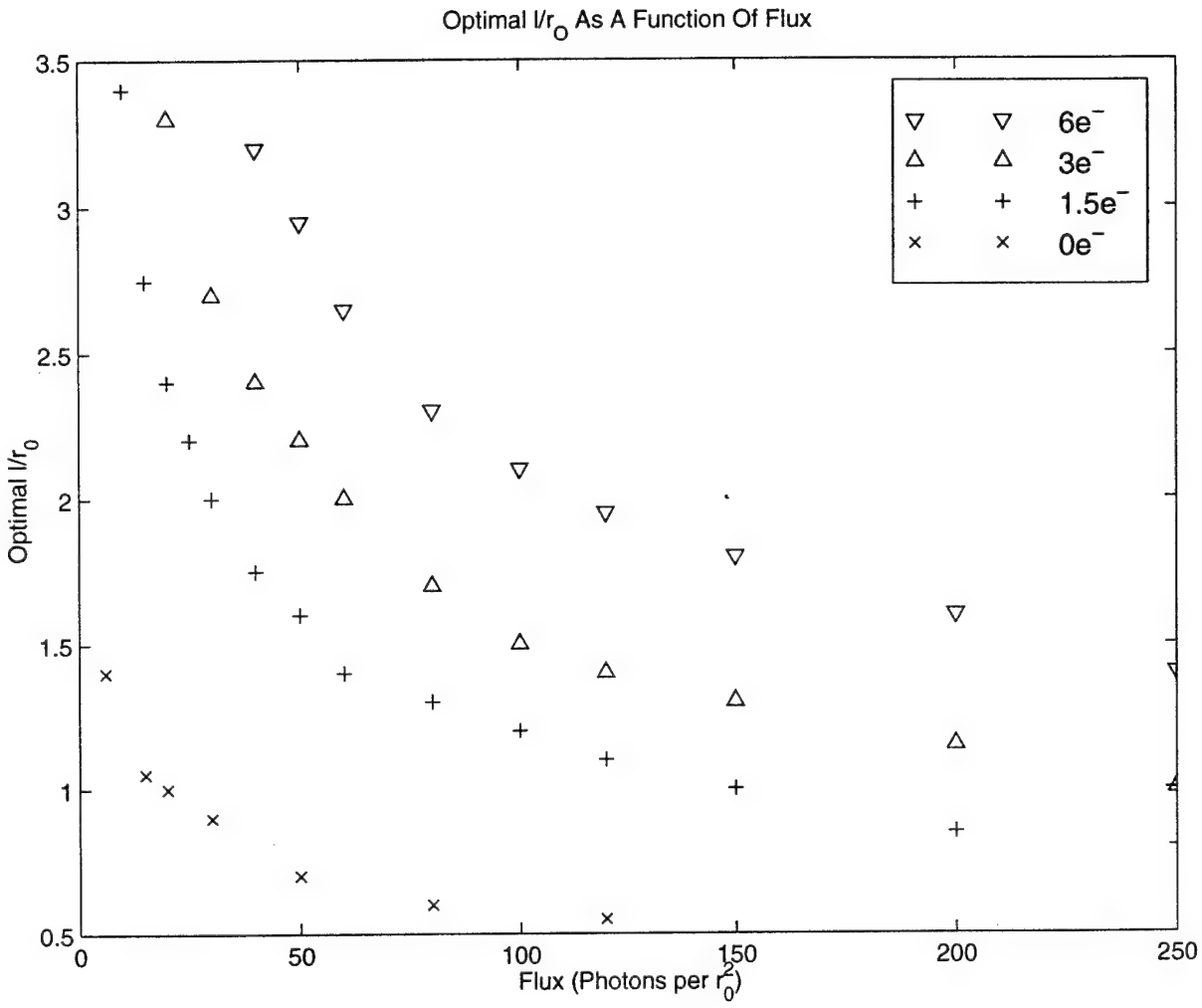
Optimal l/r0 As A Function Of Flux
Optimal l/r0
Flux (Photons per r0^2)
6e^-
3e^-
1.5e^-
0e^-
3.5
3
2.5
2
1.5
1
0.5
0
50
100
150
200
250

2. GRAM-CHARLIER EXPANSION FOR WAVEFRONT SLOPE ESTIMATION

The primary estimation task in Hartmann sensing is that of finding the barycentre (or "centroid") of the sub-aperture point-spread functions. The theory of Hartmann sensing shows that the vector shift in the position of this barycentre from that obtained with a known reference wavefront is linearly proportional to the average wavefront slope over the sub-aperture. Errors in the estimate of these slopes will propagate in a known way into the estimate of the wavefront itself and it is thus desirable that they should be kept as small as possible.

The conventional method for calculating the barycentre is to take a first moment or centre of gravity calculation on the data. Speaking generally, one of the advantages of this approach is that it makes no assumptions on the nature of the underlying distribution from which the data has been generated. However, it has problems associated with the introduction of a systematic bias and is sensitive to noise. Hartmann sensors operating with pupil-plane sub-apertures sizes of a few r_0 or less will generally produce a peaked PSF whose approximate shape may be predicted quite well. There is thus some inherent a priori information available about the underlying distribution. When signal levels are high, there is little advantage to be gained by seeking an alternative to the first moment estimator. However, in low signal-noise regimes, the sensitivity to noise becomes manifest and an estimator with better noise suppression is desirable. The following article presents results obtained with a matched filter based on modelling the PSF as a Gram-Charlier expansion. The performance is compared with the first moment estimator for a number of signal-noise scenarios.

Gram-Charlier matched filter for Shack-Hartmann sensing at low light levels

J.-M. Ruggiu and C.J.Solomon

Physics Department, University of Kent,

Canterbury, Kent CT2 7NR, U.K.

Tel:(44)01227764000 ext 3778

G. Loos

Phillips Laboratory, Kirtland Air-Force Base,

NM87117-6008 U.S.A.

October 29, 1997

A study has been made of a Gram-Charlier matched filter for Shack-Hartman sensing of wavefront slopes. The method is based on modelling the Point Spread Function (PSF) by an expansion in terms of Gauss-Hermite polynomials. We present results for several sub-aperture / coherence area sizes both with and without CCD read noise. More accurate estimation of the local slopes may be achieved at low light level as compared to the standard first moment estimator.

Keywords: Hartmann sensor, centroiding, estimation. Gram-Charlier expansion.

High quality performance in Hartmann sensors is dependent on the accurate estimation of wavefront slopes and thus on the sub-aperture centroids. This is often calculated satisfactorily by performing a first moment calculation on the sub-aperture intensity distribution. However, at low flux levels the first moment estimator for the centroid has poor noise propagation characteristics [1]. Essentially this originates from the fact that no assumptions or constraints are placed on the underlying distribution from which the data has been sampled. In noisy scenarios, use of the first moment estimator will mean that pixels far from the underlying peak will make a large contribution to the moment but, as the underlying distribution is generally unimodal, these pixels will have low signal-noise ratios. This approach to estimation also has problems associated with the introduction of a systematic bias [2,3]. There is thus a clear motivation for seeking a matched filter which effectively weights the data so as to achieve better noise propagation characteristics in noisy conditions. This fact has been recognised by workers in a variety of fields including nuclear experimentation, position tracking, microscopy and fluid mechanics [4-7].

For adaptive optics applications using Hartmann sensors, approaches using artificial neural networks [8] and Maximum a Posteriori (MAP) estimation of Hartmann centroids [9] have recently been proposed. In this paper we consider a Shack-Hartmann sensor utilising a CCD array as a detector and

investigate an alternative approach to estimating the subaperture centroid. This is based on the modelling of the sub-aperture PSF as a truncated Gram-Charlier expansion [10].

We consider the light focussed onto the CCD detector from one sub-aperture of the Shack-Hartmann sensor. We will assume that this photon distribution be represented over a square matrix of N^2 pixels, with each element registering a number of detected photoelectrons. CCD read noise is simulated by adding a Poisson sampled random deviate to each element of the matrix. The spatial distribution of the photoelectrons $I(x_i, y_j)$ is then given by -

$$I(x_i, y_j) = I_0(x_i, y_j) + N(x_i, y_j) \ \ (i = 1, .., N; j = 1, ..N) \tag{1}$$

Where $N(x_i, y_j)$ is the Poisson random value having probability density -

$$P(k) = \frac{e^{-m} m^k}{k!}$$

The parameter m specifies the mean (and the standard deviation) of the noise process.

The centroid of the distribution is given by the first moment estimator:

$$c_x = \frac{\sum_{i=1}^{N} x_i I(x_i, y_j)}{\sum_{i=1}^{N} I(x_i, y_j)}, c_y = \frac{\sum_{i=1}^{N} y_i I(x_i, y_j)}{\sum_{i=1}^{N} I(x_i, y_j)}. \tag{2}$$

The Gram-Charlier expansion is a convenient method for representing near gaussian distributions [10]. We note that when Hartmann wavefront sensors are used in problems of adaptive optics and imaging through atmospheric turbulence, it is common to employ them such that the sub-aperture size (scaled to the telescope pupil plane) will generally range from approximately 1 to $3r_0$ where r_0 is the Fried coherence parameter. For sub-aperture sizes in this range, the Hartmann PSFs will generally be peaked and unimodal and may reasonably be considered as approximately gaussian in form. In our study, we have used a two-dimensional Gram-Charlier expansion of the intensity distribution $I(x, y)$ in the CCD image plane of the following form -

$$I(x.y) = G_0(x, y)\left\{1 + \sum_{i=1}^{m} \frac{a_i^{j,k} A_i^{j,k}(x, y)}{j!(i-j)!}\right\} \tag{3}$$

Where j and k are all possible coombinations such that: $j + k = i$ and $0 \leq j \leq i, 0 \leq k \leq i$. and where G_0 represents the best least-squares gaussian fit to the distribution I(x,y):

$$G_0(x, y) = \alpha e^{-\left\{\frac{(x-u)^2}{2\sigma_x^2}) + \frac{(y-v)^2}{2\sigma_y^2}\right\}} \tag{4}$$

The free parameters α, u,v σ_x and σ_y for the gaussian fit are found by minimising a standard χ^2 error metric -

$$\chi^2(\alpha, u, v, \sigma_x, \sigma_y) = \sum_{i=1}^{N}\sum_{j=1}^{N} [I(x_i, y_j) - G_0(x_i, y_j)]^2 \tag{5}$$

The $A_i^{j,k}$ functions are defined as -

$$A_i^{j,k}(x, y) = H_j(x)H_k(y), \quad j + k = i, 0 \leq j \leq i, 0 \leq k \leq i \tag{6}$$

where the H^j represent the Hermite polynomials. The Hermite polynomials are a complete orthogonal set over the real axis with respect to the weight function $e^{-\frac{x^2}{2}}/\sqrt{2\pi}$. Thus,

$$\begin{aligned} < H^j, H^k > &= \frac{1}{\sqrt{2\pi}} \int_R e^{-\frac{x^2}{2}} H_j(x) H_k(x) dx \\ &= j! \delta_{jk} \end{aligned} \tag{7}$$

The $A_i^{j,k}$ are two dimensional polynomials of degree i=j+k and are a complete orthogonal set over the space of all real number pairs, R[X,Y] -

$$\begin{aligned} < A_i^{j,k}, A_{i'}^{j',k'} > &= \int_R \int_R \frac{e^{-\frac{x^2+y^2}{2}}}{2\pi} H_j(x) H_{j'}(x) H_k(y) H_{k'}(y) dx dy \\ &= j!k! \delta(j-j') \delta(k-k') \end{aligned} \tag{8}$$

The coefficients in the expansion described by eq.3 are thus given by evaluating the integral -

$$a_i^{j,k} = \int_R \int_R \frac{e^{-\frac{x^2+y^2}{2}}}{2\pi} \left(\frac{I(x,y)}{G_0(x,y)} - 1 \right) A_i^{jk}(x,y) dx dy \tag{9}$$

which in discrete form becomes -

$$a_i^{j,k} = \sum_{l=1}^{N} \sum_{p=1}^{N} \frac{e^{-\frac{x_l^2+y_p^2}{2}}}{2\pi} \left(\frac{I(x_l,y_p)}{G_0(x_l,y_p)} - 1 \right) A_i^{jk}(x_l,y_p) \tag{10}$$

A computer simulation was performed to compare the Gram-Charlier matched filter and first moment methods for estimating the sub-aperture PSF centroid. Wavefronts were generated having statistics that obey the Kolmogorov model [11] and the resulting reference (i.e. infinite light level) sub-aperture

PSFs were generated. The precise centroid of these reference PSFs was then calculated. Taking the infinite light level PSF as an unnormalised probability density, the PSFs were then photon-sampled using standard techniques and CCD read noise was added to produce a sub-aperture photon distribution. The centroid of this distribution was then calculated using both the first moment estimator and the Gram-Charlier method and compared against the exact value calculated from the reference PSF. A comparison was made for three sub-aperture size ratios of $\frac{l}{r_0} = 1,2$ and 3. A mean signal level of 30 photoelectrons per sub-aperture was used in all cases. Read noise was simulated using a Poisson model at a level of 1.5 electrons r.m.s per pixel per frame. The simulation was configured such that the generated PSFs were contained within an area of 3*3 CCD pixels [12]. This area was located and the first moment estimation of the centroid was performed.

• Figure 1 compares the two estimators for the situation in which no detector read noise is added to the sampled data. The data points corresponding to the ordinate labelled -1 represent the rms error in CCD pixels of the centroid from use of the first moment estimator and the data points at the ordinate 0 represent the rms error resulting from a least squares Gaussian fit to the data. Data points at subsequent integer values of the ordinate give the rms error as the radial order of the Gauss-Hermite fit is increased. The graph shows an improvement (~15%) for the Gaussian and first order Hermite functions. We see that adding more terms does not significantly affect the accuracy.

• Figure 2 was generated under similar conditions to figure 1 but compares the two estimators when simulated CCD read noise has been added to the photon limited data. This graph confirms that the gaussian matched filter yields a significant improvement in the slope estimate. Addition of the first order Hermite terms yields a further minor gain after which the higher order terms reduce the accuracy. This behaviour is intuitively expected since the fitting of higher order terms will increasingly tend to reproduce the noise. It is also consistent with the fact that their contribution was negligible in figure 1 where no read-noise was present.

• Figure 3 illustrates the estimation procedure graphically using contour plots. A high light level Hartmann subaperture image (first row: left) is sampled for 30 photoelectrons and CCD read noise added using a mean level of 1.5 electrons r.m.s per pixel per frame (first row: middle). The result of performing a gaussian fit (first row: right) is followed by fits including successively higher order Hermite terms.

• Table 1 compares some corresponding r.m.s wavefront errors for the first moment estimator and for the Gram-Charlier method. Results are given for the least-square and MAP reconstructors [14,15] for a number of different operating conditions. We see that as the signal decreases, the gain of the Gram-Charlier estimator over the first moment estimator increases.

We have investigated a matched filter for Shack-Hartmann slope estimation at low light levels based on a truncated Gram-Charlier expansion. The

orthogonality of the functions allows independent and direct evaluation of the coefficients by integration. Our results indicate that a significant increase in accuracy over the standard first moment/centre of gravity estimator can be made for subaperture sizes from $1 - 3r_0$. A recent study of low-light level wavefront sensing suggests that the optimum subaperture size will generally fall within this region [13].

In the calculation of the Gram-Charlier coefficients we found it necessary to restrict the region of integration indicated by eq. 11 to a region within approximately 2.5 standard deviations about the centre of the Gaussian fit. The presence of noise means that integration over a larger interval results in instability in the Gram-Charlier coefficients. In the current work, the appropriate domain of integration has been established on an empirical basis. We note that Bayesian MAP estimation techniques have been successfully applied both to centroid and to wavefront estimation [9.14] and these should provide a natural way of allowing the domain of the fitting procedure to be extended whilst constraining the estimated coefficients. Such an approach requires that a large ensemble of high light level subaperture PSFs be measured to generate prior knowledge in the form of an ensemble covariance of the Gram-Charlier coefficients.

The authors would like to acknowledge the support provided by the European Office of Aerospace Research and Development (SPC-96-4054) and the U.K. Engineering and Physical Sciences Research Council (GR/L26339).

References

1. N. Dillon, "PWFS Signal Processing algorithms", *Gemini A & G System technical report*,(1995).

2. B. F. Alexander and K. C. Ng, Opt. Eng. **30**, 1320 (1991).

3. I. E. Abdou, Opt. Eng. **34** (1995).

4. M. Chemloul and V. Comparat, Nucl. Inst. Meth. A **367**, 290 (1995).

5. R. Baribeau and M. Rioux, Appl. Opt. **30**, 3752 (1991).

6. A. Patwardhan, Journal of Microscopy **186**, 246 (Oxford 1997).

7. M. P. Wrenet and A. Pline, Experiments in Fluids **15**, 295 (1993).

8. D. A. Montera, B. M. Welsh, M. C. Roggeman and D. W. Ruck, Appl. Opt., **35**, 5747 (1996).

9. S. A. Sallberg, B. M. Welsh and M. C. Roggemann, J. Opt. Soc. Am. A **14**, 1347 (1997).

10. B.R. Frieden, *Probability, Statistical Optics, and Data Testing*, 2nd edition (Springer-Verlag 1991).

11. R.J. Noll, J. Opt. Soc. Am. A, **66**. 207 (1976).

12. K.A. Winick, J. Opt. Soc. Am. A, **3**, 1809 (1986).

13. D.L. Ash and C.J. Solomon in *Proceedings of 1997 SPIE Annual Meeting* (International Symposium on Optical Science, Engineering. and Instrumentation, San Diego, 1997), paper 3126-37 (to be published).

14. C.J. Solomon, N.J. Wooder and J.C. Dainty, Opt. Rev.. **2**, 217 (1995).

15. T. O. Lewis and P. L. Odell,*Estimation in Linear Models*, (Prentice-Hall 1971).

Figure1: Mean-square error in centroid estimate using the first moment estimator and for different orders (0 to 6) of the Gram-Charlier fit. The flux level is 30 photoelectrons per sub-aperture. No read-noise is present and $\frac{l}{r_0}$ varies from 1 to 3.

Figure2: Mean-square error in centroid estimate using the first moment estimator and for different orders (0 to 6) of the Gram-Charlier fit. The flux level is 30 photoelectrons per sub-aperture. Poisson read-noise is added and $\frac{l}{r_0}$ varies from 1 to 3.

Figure3: Graphical illustration of the effect of adding more Gram-Charlier terms: Initially, the centroid estimate improves but the addition of too many terms tends to reproduce the noise.

Table 1: R.m.s. wavefront reconstruction error for the first moment and Gram-Charlier estimators. Thee results are calculated for two wavefront reconstructors: least-squares (zrms) and MAP (maprms).

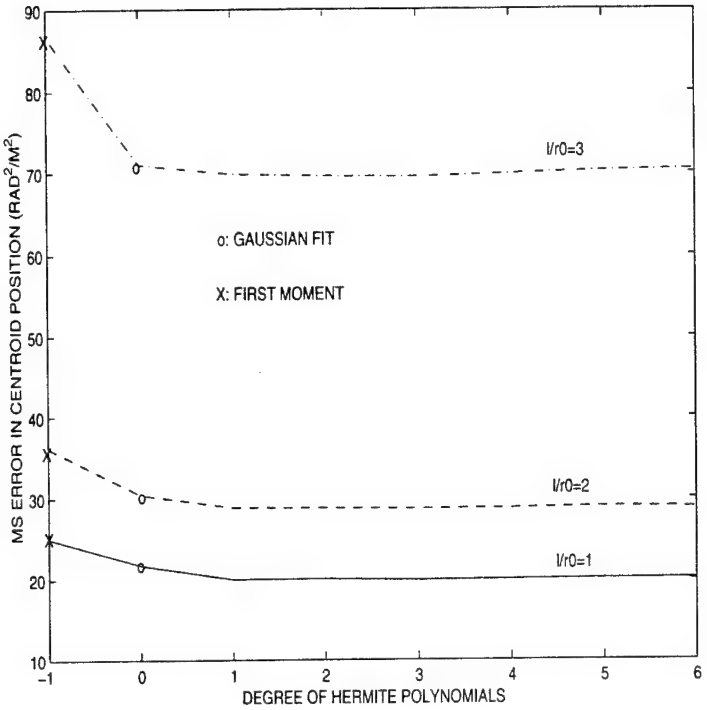
MS ERROR IN CENTROID POSITION (RAD^2/M^2)
DEGREE OF HERMITE POLYNOMIALS
l/r0=3
l/r0=2
l/r0=1
o: GAUSSIAN FIT
X: FIRST MOMENT
90
80
70
60
50
40
30
20
10
−1
0
1
2
3
4
5
6

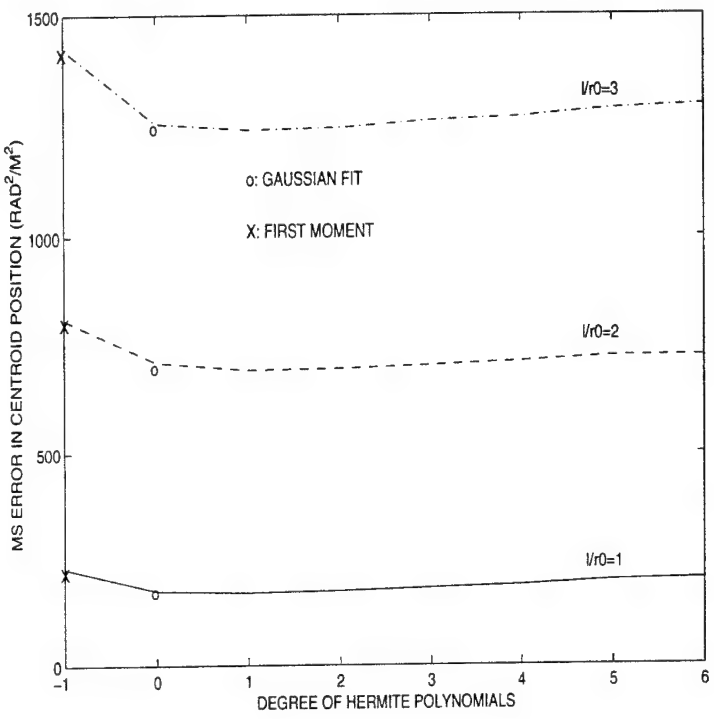
1500
1000
500
0
−1
0
1
2
3
4
5
6
MS ERROR IN CENTROID POSITION (RAD²/M²)
DEGREE OF HERMITE POLYNOMIALS
o: GAUSSIAN FIT
X: FIRST MOMENT
l/r0=3
l/r0=2
l/r0=1

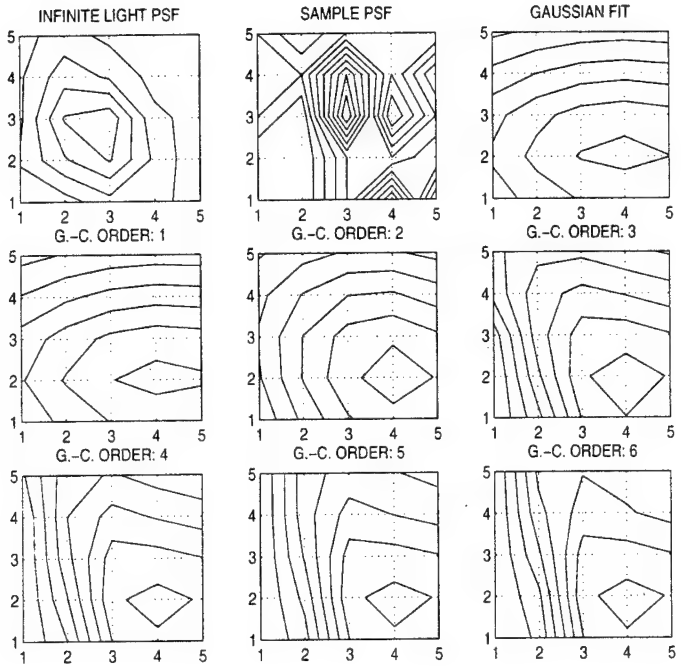
INFINITE LIGHT PSF
SAMPLE PSF
GAUSSIAN FIT
G.-C. ORDER: 1
G.-C. ORDER: 2
G.-C. ORDER: 3
G.-C. ORDER: 4
G.-C. ORDER: 5
G.-C. ORDER: 6

l/r_0	r_0 (m)	D (m)	Number of subapertures	Flux (p.e./r_0^2 /frame) Exposure time =5 ms	Corresponding Visual Magnitude	A priori phase variance ($1.015\ (D/r_0)^{5/6}$ rad)	R.m.s Error (rad) 1st moment estimator	R.m.s Error (rad) Gram-Charlier estimator
1	0.1	0.7	32	30	10.73	5.14	zrms=1.29190 maprms=1.0356	zrms=1.1189 maprms=0.973
2	0.1	1.3	32	7.5	12.24	8.61	zrms=4.1890 maprms=2.8663	zrms=3.8648 maprms=2.7052
3	0.08	1.6	32	3.33	12.63	12.32	zrms=7.3787 maprms=4.8561	zrms=6.8812 maprms=4.6128
1	0.1	1.3	124	30	10.73	8.61	zrms=1.0612 maprms=1.0265	zrms=0.9191 maprms=0.8967
2	0.08	2.1	124	7.5	11.75	15.46	zrms=3.2369 maprms=2.9700	zrms=2.9914 maprms=2.7733
3	0.08	3.2	124	3.33	12.63	21.95	zrms=6.5272 maprms=5.6489	zrms=6.0866 maprms=5.3383

3. BAYESIAN ESTIMATION, MODAL PROJECTION AND SENSOR GEOMETRY

A maximum a posteriori (MAP) Bayesian wavefront estimator was derived in section 1 of the interim report[1]. The error covariance matrix of this estimator was derived and evaluated for a number of typical Hartmann imaging scenarios and compared to the best linear unbiassed estimator (BLUE). The derivation and explicit method of evaluation is not therefore repeated here. Results obtained from this are given in figs 3.1 - 3.3. Significant gains are apparent at low flux levels. These results do not include the effects of detector noise (for example CCD read noise) as it is difficult to analytically incorporate this into the noise model. However, the basic trend of these results which indicates a significant improvement at low light levels can be expected to appear when detector noise is present.

The superior performance of the MAP estimator is dependent on having the correct form for the a priori atmospheric phase covariance matrix, C. Non-Kolmogorov behaviour of the atmosphere would therefore require an experimentally determ ined form for the covariance rather than a theoretical/analytical one.

The issue of sensor geometry received some discussion in the early literature [2-6] where the conclusion was reached that the wavefront error is fairly insensitive to sensor geometry (in the sense of size and placement of subapertures). For this reason, most Hartmann sensors use the simple and practical "square-grid" geometry giving a uniform sampling over the pupil. Recent work [7,8] has suggested however, that gains can potentially be made by combining a Hartmann geometry conforming to the Albrecht cubature nodes with a suitably constructed set of vector polynomials to estimate wavefront modes by direct integration. To see how this is achieved in principle, it is necessary to first introduce a set of vector polynomials which can restore the orthogonality of the linear problem that arises in Hartmann sensing.

3.1 Vector polynomials orthogonal to the gradient of the basis functions

In problems of wavefront estimation, it is common to expand the wavefront in terms of a set of orthogonal functions. The most common of these, of course, are the Zernike circular polynomials. Speaking generally, orthogonal bases are often desirable because they allow the expansion coefficients to be evaluated by simple integration of a product of two functions over the domain. However, since Hartmann sensors (and shearing interferometers) provide estimates of the *gradient of the phase* rather than the phase itself, the orthogonality of, for example the Zernike or Karhunen-Loeve basis cannot be exploited. Modal cross-coupling can occur and coefficients must be obtained by solving a least-squares procedure.

Consider the wavefront to be expanded in terms of an orthogonal set of modes -

$$\Phi(\underline{x}) = \sum_{k=1}^{N} a_k P_k(\underline{x}) \tag{3.1}$$

Slope-based wavefront sensing implies that our model is thus -

$$\langle \nabla \Phi(\underline{x}_j) \rangle = \sum_{k=1}^{N} a_k \langle \nabla P_k(\underline{x}_j) \rangle \tag{3.2}$$

The evaluation of modes by direct integration could be restored if we can derive a set of auxiliary functions $\vec{F}_i(\underline{x})$ which are *orthogonal to the gradients of the basis functions.*

Let these functions obey the relation -

$$\vec{\nabla} \cdot \vec{F}_i(\underline{x}) = P_i(\underline{x}) \tag{3.3}$$

where the orthogonality relation for the basis is -

$$\int_D P_i(\vec{x}) P_j(\vec{x}) d^2x = \delta_{ij} \tag{3.4}$$

and D denotes the domain of integration.

Using the orthogonality of the basis in eq. 3.1 and substituting eq. 3.3, the modal coefficients are given by -

$$a_i = \int_D \phi(\underline{x}) P_i(\underline{x}) d^2x = \int_D \phi(\underline{x}) \vec{\nabla} \cdot \vec{F}_i(\underline{x}) d^2x$$

This may be written as -

$$a_i = \int_D \vec{\nabla} \cdot (\vec{F}_i(\underline{x}) \cdot \phi(\underline{x})) d^2x - \int_D \vec{\nabla} \phi(\underline{x}) \cdot \vec{F}_i(\underline{x}) d^2x$$

and applying the divergence theorem, we obtain -

$$a_i = \oint_C \phi(\underline{x}) \vec{F}_i(\underline{x}) \cdot \vec{dl} - \int \vec{\nabla} \phi(\underline{x}) \cdot \vec{F}_i(\underline{x}) d^2x \tag{3.5}$$

If the required set of functions $\vec{F}_i(\underline{x})$ obeys -

$$\vec{\nabla} \cdot \vec{F}_i(\underline{x}) = P_i(\underline{x})$$

$$\vec{F}_i(\underline{x})|_n(C) = 0 \tag{3.6}$$

where $F_i(\underline{x})|_n(C)$ denotes the normal component of the function to the closed contour C of the integration domain D, we then have -

$$a_i = -\int_D \vec{\nabla} \phi(\underline{x}) \cdot \vec{F}_i(\underline{x}) d^2x \tag{3.7}$$

and we may evaluate the modes by *direct integration* as required.

There are in fact a number of possible sets of vector polynomials which are orthogonal to the gradient of the Zernike basis [7,9,10]. This is because there is no unique solution to eq. 3.3 with the given boundary conditions eq. 3.6. Here, we make use of the set originally derived by Gavrielides and refer the reader to the original source for the derivation[9]. In the appendix A3, we prove that these functions are *irrotational and minimum norm.* This property of the functions appears to have been unknown until now but is important because it guarantees that of all possible sets of vector polynomials orthogonal to the gradient of the basis functions, they will have the *smallest noise propagation.* For completeness, the explicit form for generation of the Gavrielides functions in polar coordinates and the corresponding error covariance (noise propagation) for the modal estimator described by eq. 3.7 are also given in the appendices A1 and A2.

3.2 Noise propagation and Sensor geometry

By making use of the Gavrielides polynomials, the modal coefficients can be estimated by direct integration over the pupil according to eq. 3.7. We point out that restoration of the orthogonality via Gavrielides functions allows us to estimate the "pure" modal content of a distorted wavefront. In other words, the contribution of each mode is estimated independently of the others. For a non-orthogonal problem, least-squares solutions effectively allow a shuffling of modes (in a manner analogous to aberration compensation in optical design) so as to achieve the minimum norm error with respect to the data. However, as far as minimising the mean-square wavefront error there is no advantage per se in transforming to an orthogonal basis. This has been noted by Southwell [9]. Any advantage must come as the result of sampling the pupil plane in a way which gives reduced noise on the calculations which are required to estimate the modes.

In Hartmann sensing, we do not have the continuous function $\nabla\phi(\underline{x})$ but rather have it's value at a number of sample points. The simplest approach to estimating the modes using the auxiliary vector functions (and a reasonable one for a regular Hartmann geometry) is to approximate the integral by a simple two-dimensional summation -

$$a_i = -\sum_j \vec{\nabla}\phi(\underline{x}_j) \cdot \vec{F}_i(\underline{x}_j) dA \tag{3.8}$$

where the area element dA is simply equal to the area of the pupil (π divided by the total number of sample points (sub-apertures)).

There is a large literature devoted to efficient and accurate numerical integration of functions sampled over closed domains. In general, these schemes will attempt to identify those points at which smooth functions (typically polynomials) need to be sampled within the given domain in order that they may be integrated most accurately. The cubatures

which we have used in this study are due to Albrecht and Engels [11] and define a set of x,y points lying within a circular domain with each of which we associate a weight so that we approximate the integral by finite sums of the form -

$$a_k = -c_k^{-1} \sum_{\alpha=1}^{N} w_\alpha f_\alpha \vec{\nabla}\phi(\alpha) \cdot \vec{F}_k(\alpha) \tag{3.9}$$

$\alpha = 1 \rightarrow N$ labels the points at which the integrand is evaluated (known as the nodes of the cubature), w_α are the weights associated with these points and f_α is 1 if cartesian coordinates are used and r_α if polar coordinates are used.

In the appendix A2, the mean-square error resulting from use of the estimator in eq. 3.8 is derived. It is given in matrix form by -

$$\sigma^2 = Tr\left\{[F^T V^{-1} F + C_x^{-1}]^{-1}\right\} \tag{3.10}$$

The mean square error resulting from use of the Albrecht's grid geometry is given by

$$\sigma^2 = -c_k^{-2} \sum_{\alpha=1}^{N} w_\alpha^2 f_\alpha^2 \vec{F}_k(\alpha) \cdot \vec{F}_k(\alpha) \tag{3.11}$$

This error covariance matrix was generated using Gavrielides functions and both the regular square Hartmann geometries and Albrecht's grid geometries for several signal-noise/turbulence scenarios. Also compared were the errors on the individual modes for the MAP bayesian estimator and the BLUE estimator. Our studies have shown that although the use of the MAP estimator results in reduced noise propagation (see figs. 3.4 - 3.6) for 32, 43 and 80 subapertures respectively, the geometrical arrangement of subapertures does not appear to have a significant effect on the noise propagation.

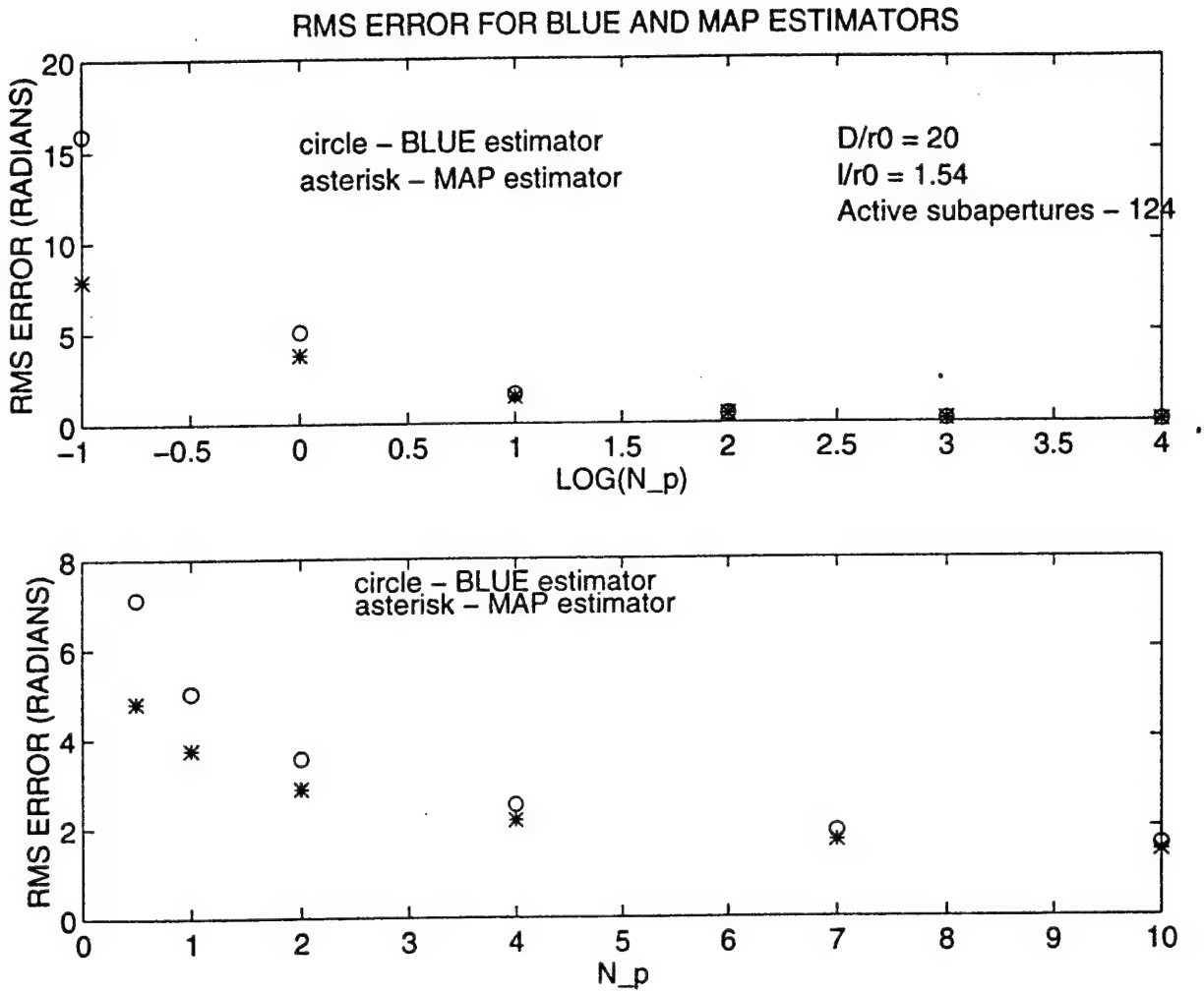

FIGURE 3.1

r.m.s. wavefront error against photoelectron signal in each sub-aperture.

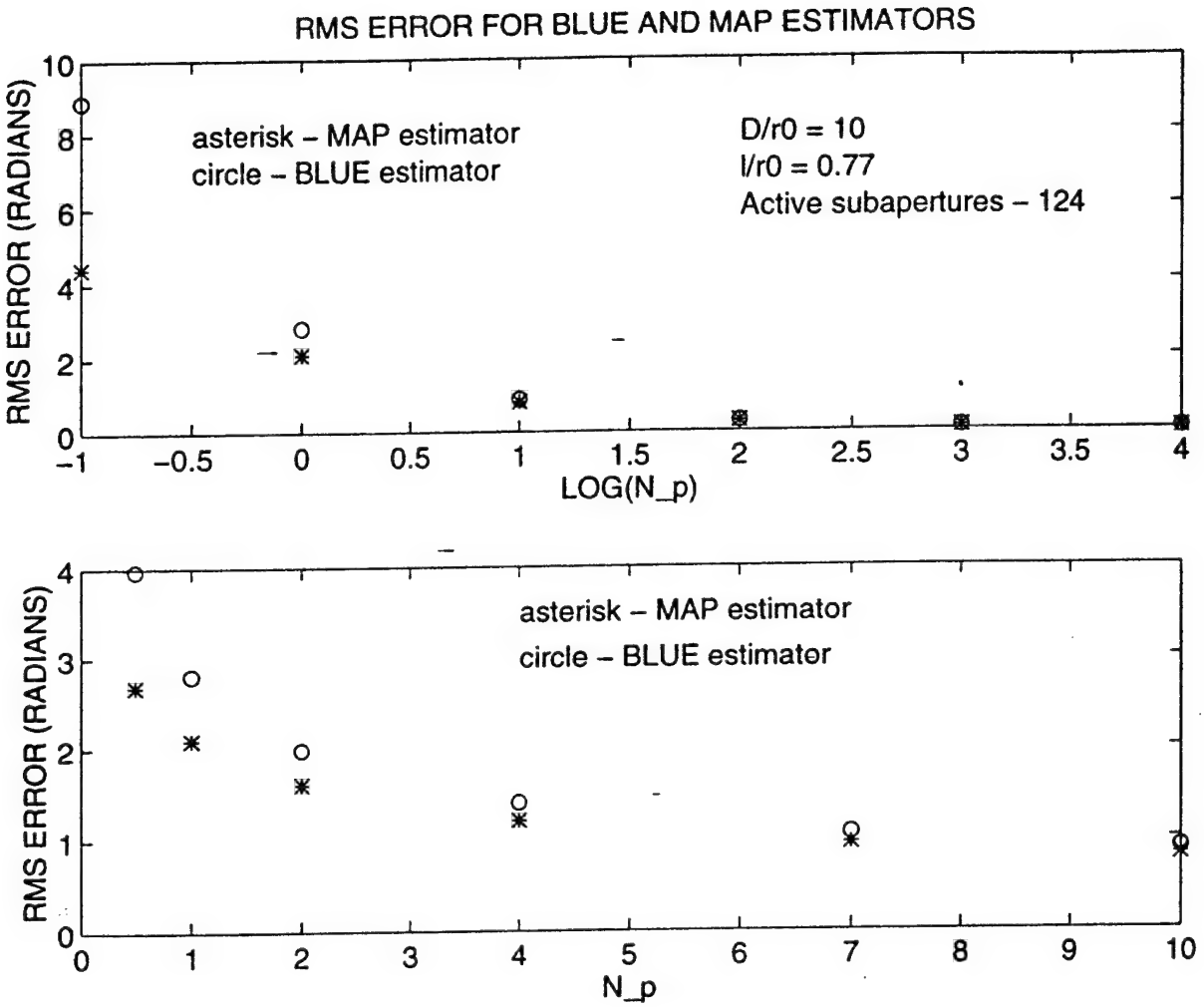

FIGURE 3.2

r.m.s. wavefront error against photoelectron signal in each sub-aperture.

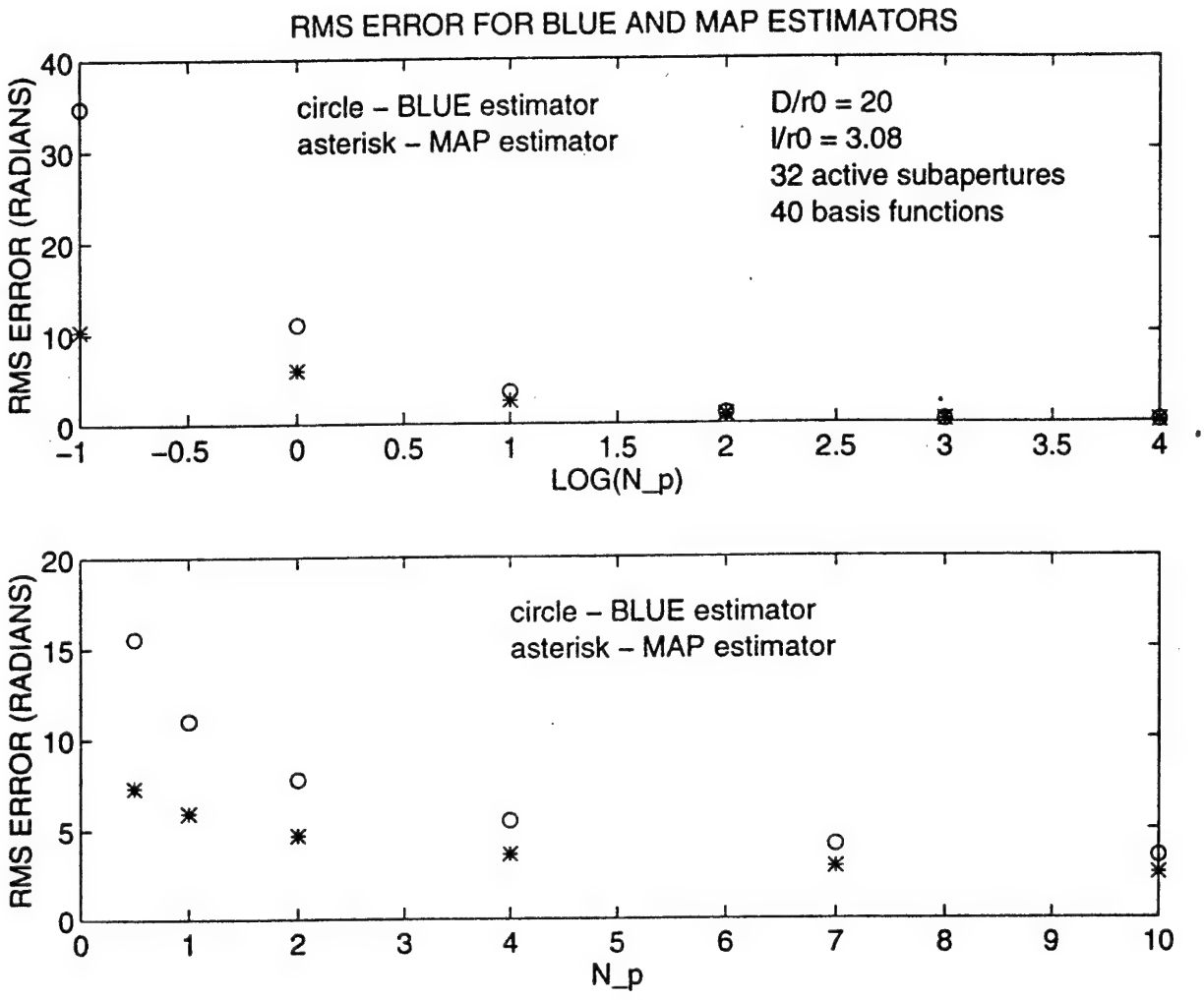

FIGURE 3.3

r.m.s. wavefront error against photoelectron signal in each sub-aperture.

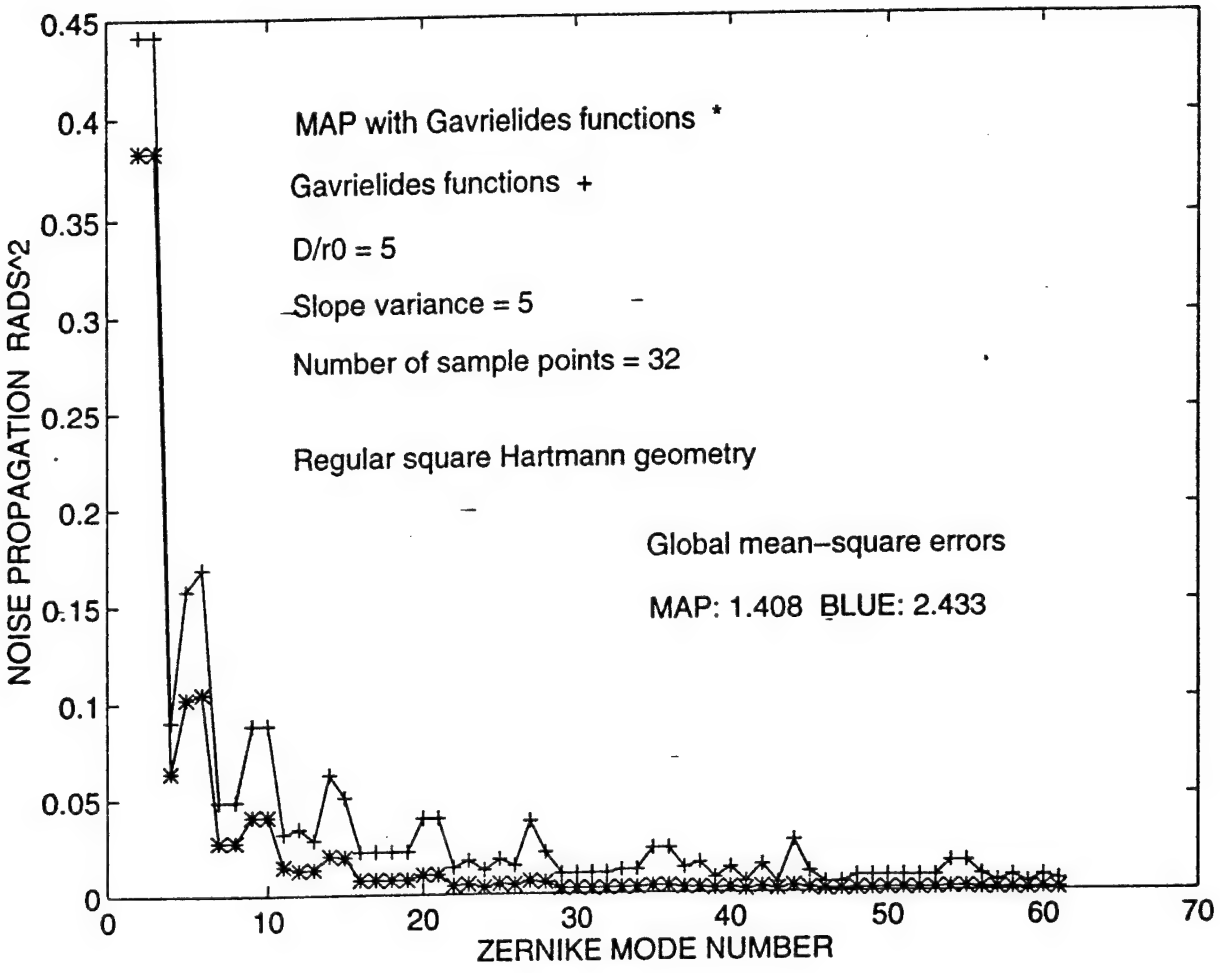

FIGURE 3.4

Noise propagation on the individual Zernike modes for the Gavrielides functions with regular Hartmann geometry.

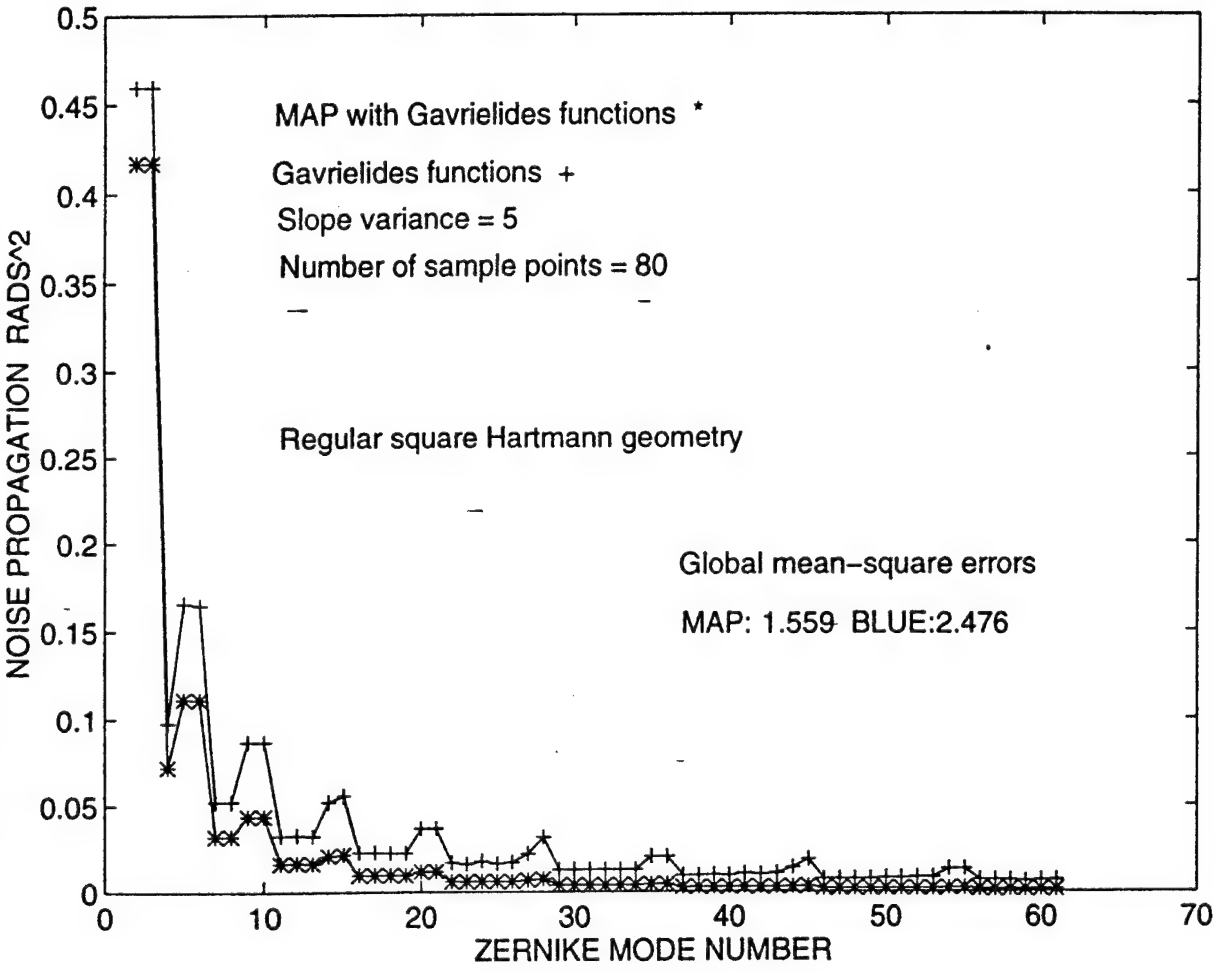

FIGURE 3.5

Noise propagation on the individual Zernike modes for the Gavrielides functions with regular Hartmann geometry.

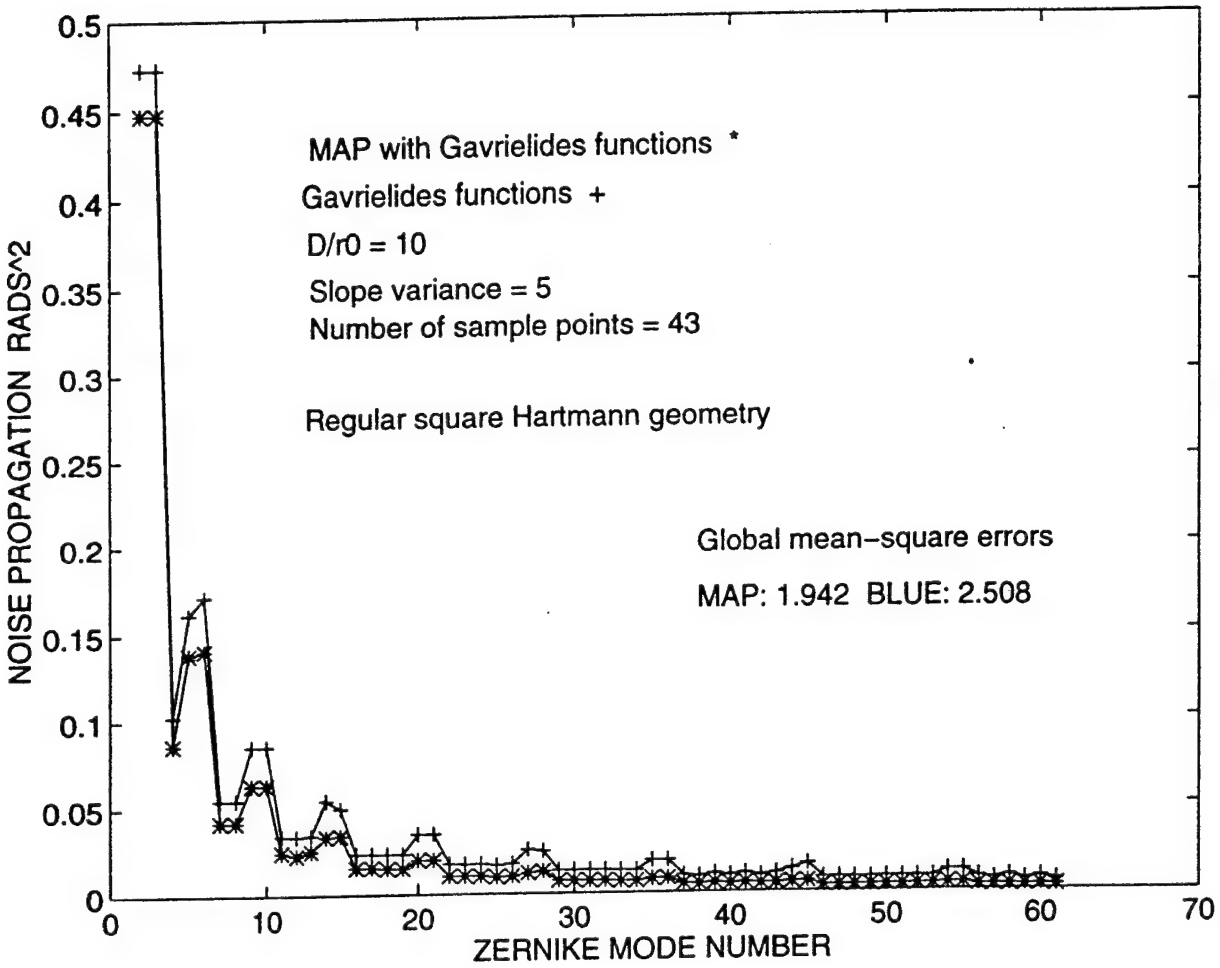

FIGURE 3.6

Noise propagation on the individual Zernike modes for the Gavrielides functions with regular Hartmann geometry. The Bayesian MAP solution has better noise propagation than the BLUE.

References

1. C.J. Solomon, March 1997. Optimal Shack-Hartmann wavefront sensing for low light levels. Interim report, E.O.A.R.D. SPC-96-4054.

2. R. Cubalchini, " Modal wavefront estimation from phase derivative measurements ", J. Opt. Soc. Am., Vol 69, 972-977, (1979)

3. W.H. Southwell, Wavefront estimation from wavefront slope measurements, J. Opt. Soc. Am., Vol 70, No. 8, (1980)

4.. R.H. Hugdin, Wavefront reconstruction for compensated imaging, J. Opt. Soc. Am., Vol 67, 375-378, (1977)

5. J. Herrmann, Least-squares wavefront errors of minimum norm , J. Opt. Soc. Am., Vol 70, 28-35, (1980)

6. D.L. Fried, " Least square fitting a wavefront distortion to an array of phase difference measurements ", J. Opt. Soc. Am.,Vol 67, 370-375, (1977)

7. S. Rios, E. Acosta and S. Bara 1997. Hartmann sensing with Albrecht's grids. Opt . Comm. 133, pp443-453.

8. S. Bara, S. Rios and E. Acosta 1996. Integral evaluation of the modal phase coef ficients in curvature sensing: Albrecht's cubatures. J. Opt. Soc. Am. A, Vol 13, No. 7, (199 6).

9. A. Gavrielides, "Vector polynomials orthogonal to the gradient of the Zernike polynomials", Opt. Lett. 11, 526-529 (1982)

10. W.H. Southwell, "What's wrong with cross-coupling in modal wavefront estimation ?", Proc. Soc. Photo-opt. Instrum. Eng. 365, 97, (1982).

11. H. Engels, "Numerical quadrature and cubature", Academic Press, (1980).

12. R.J. Noll, 1976. Zernike polynomials and atmospheric turbulence. J. Opt. Soc. Am. **66**, 207-211.

4: SUMMARY

4.1 Optimal subaperture size for Hartmann sensors

A study has been made of optimising the Hartmann sub-aperture size for wavefront sensing applications at low light levels and submitted for publication to Optics Communications. This is based on a detailed computer model simulating the effects of turbulence, Poisson and CCD read noise on the wavefront sensing process. Our results demonstrate that optimal wavefront estimation and correction is critically dependent on matching the sub-aperture size to the prevailing signal-noise ratio and we give the optimal values for a number of typical low light level imaging scenarios.

4.2 Gram-Charlier centroid estimation

A study has been made of a Gram-Charlier matched filter for the estimation of Shack-Hartmann sub-aperture barycentres at low light levels. The results of this work have been submitted and accepted for publication in Optics Letters. A significant increase in accuracy over the standard first moment/centre of gravity estimator can be made when the subaperture size is $2 - 3r_0$. The residual mean-square error in the wavefront estimate has been calculated and the limiting visual magnitude at which this performance may be achieved has been calculated for a number of imaging conditions.

4.3 Bayesian and modal projection estimation

We have derived and implemented a Bayesian estimator for reconstruction of atmospherically perturbed wavefronts. The prior knowledge is implemented in this estimator by assuming that the atmosphere induces phase fluctuations obeying the Kolmogorov power spectrum. The covariance matrix for the atmospheric modes thus obeys the form originally derived by Noll [1]. Calculations of the error covariance matrix for a number of different sub-aperture sizes $\frac{l}{r_0}$ and a number of different turbulence strengths have indicated that the Bayesian estimator has a reduced mean-square error as compared to the standard least-squares estimator. This improvement is particularly significant at low signal levels. These results are presented and discussed fully in the interim report[1].

We have also investigated a method of modal projection estimation based on direct integration using a set of auxiliary vector polynomials which are orthonormal to the gradients of the Zernike polynomials. This is a quick and convenient procedure which ensures that the modes are estimated individually without modal cross-coupling. However, since adaptive optics applications are generally concerned with minimising the *global* mean square wavefront error (rather than errors on particular individual modes) we have examined the overall noise propagation of this method when combined with the Albrecht's

cubatures defined on the unit radius circle. We have developed a Bayesian estimator using the auxiliary vector polynomials and have shown that the noise propagation is superior to that obtained by direct modal projection in which no a priori knowledge is incorporated. Although there is some computational advantage in using the auxiliary vector polynomials, our study suggests that the use of tailored Hartmann sub-aperture geometries has no significant effect on noise propagation and will not lead to reduced mean-square error in wavefront estimation as compared to the regular Hartmann geometry.

APPENDICES

A1 : GAVRIELIDES' POLYNOMIALS

These vector polynomials are orthonormal with respect to the gradient of the Zernike polynomials. They are defined in polar coordinates as -

1. $m \neq 0$

$$F_\rho^i = \frac{1}{\pi}\sqrt{2(n+1)}T_n^m(r)\begin{cases} cosm\theta & ifieven \\ sinm\theta & ifiodd \end{cases}$$

$$F_\theta^i = \frac{1}{\pi}\sqrt{2(n+1)}Q_n^m(r)\begin{cases} -msinm\theta & ifieven \\ mcosm\theta & ifiodd \end{cases}$$

where:

$$T_n^m(r) = \frac{1}{4}\sum_{s=0}^{\frac{n-m}{2}} \frac{C_n^m(s)\,(n-2s+2)\,[r^{m-1} - r^{n-2s+1}]}{\left(\frac{n+m}{2}-s+1\right)\left(\frac{n-m}{2}-s+1\right)} \tag{1}$$

$$Q_n^m(r) = \frac{1}{4m}\sum_{s=0}^{\frac{n-m}{2}} \frac{C_n^m(s)\,[(n-2s+2)\,r^{m-1} - mr^{n-2s+1}]}{\left(\frac{n+2}{m}-s+1\right)\left(\frac{n-m}{2}-s+1\right)} \tag{2}$$

2. m=0

$$F_\rho^i = \frac{1}{\pi}\sqrt{n+1}\sum_{s=0}^{\frac{n}{2}} \frac{(-1)^s(n-s)!r^{n-2s+1}}{s!\left[(\frac{n}{2}-s)!\right]^2(n-2s+2)} \tag{3}$$

$$F_\theta^i = 0 \tag{4}$$

A2: NOISE PROPAGATION FOR GAVRIELIDES' FUNCTIONS

Our model for the wavefront is a finite expansion in terms of a known set of basis functions. Accordingly, we begin from the discretised linear system given in eq. 1.4 -

$$Ax + \epsilon = m \tag{5}$$

where x is the N by 1 vector of unknown modal coefficients, A is the system or design matrix of size M by N and containing the gradients of the basis functions evaluated at the sensor positions, m is the M by 1 phase gradient measurement vector and e is the error vector. We make identical assumptions on this model to those outlined in section 1. Let us apply a linear transformation to this system of equations by applying a matrix F^T from the left on both sides -

$$F^T Ax + F^T \epsilon = F^T m \tag{6}$$

The result is also a matrix-vector equation which we denote -

$$\tilde{A}x + \tilde{\epsilon} = \tilde{m} \tag{7}$$

So, we seek a linear estimator $\hat{x} = Lm$ which will minimise the error covariance matrix P defined by -

$$P = \langle (x - \hat{x})(x - \hat{x})^T \rangle \tag{8}$$

We substitute $\hat{x} = L(\tilde{A}x + \tilde{\epsilon})$ in eq. 8 to obtain -

$$P = [I - L\tilde{A}]C_x[I - L\tilde{A}]^T + L\tilde{V}L^T \tag{9}$$

where $\tilde{V} = \langle \tilde{\epsilon}\tilde{\epsilon}^T \rangle = F^T V F$ Taking variations in matrix P with respect to L and setting to zero, we have -

$$\delta P = \delta L(\tilde{A}C_x[I - L\tilde{A}]^T + \tilde{V}L^T) + ([I - L\tilde{A}]C_x\tilde{A}^T + L\tilde{V})\delta L^T = 0 \tag{10}$$

which yields an optimal matrix L -

$$L_{MAP} = L = C_x\tilde{A}^T[\tilde{A}C_x\tilde{A}^T + \tilde{V}]^{-1} \tag{11}$$

Substitution of $\hat{x} = L_{MAP}\, m = L_{MAP}(\check{A}x + \check{e})$ into eq.4 defining P yields an error covariance matrix given by -

$$P_{MAP} = C_x[I - \check{A}^T[\check{A}C_x\check{A}^T + \check{V}]^{-1}\check{A}C_x] \tag{12}$$

In appendix A, we show the equivalence of eqs 11 and 12 to the following two forms -

$$\hat{x} = L_{MAP}\, m = [\check{A}^T\check{V}^{-1}\check{A} + C_x^{-1}]^{-1}\check{A}^T\check{V}^{-1}\check{m} \tag{13}$$

$$P = P_{MAP} = [\check{A}^T\check{V}^{-1}\check{A} + C_x^{-1}]^{-1} \tag{14}$$

Now suppose that we are able to construct a set of functions (represented in sampled form by the columns of the matrix F) which are orthogonal to the gradient of the basis functions (i.e. the Gavrielides' functions). In other words, we are able to find a matrix such that $F^TA = I$, the identity matrix. Since we derived equations 13 and 14 for a quite general matrix F, we may then simply substitute back $\check{A} = F^TA$, $\check{e} = F^Te$ and $\check{m} = F^Tm$ into eqs 13 and 14 to obtain an estimator for the modal coefficients -

$$\hat{x} = F^Tm \tag{15}$$

with an associated error covariance of -

$$P = P_{MAP} = [(F^TVF)^{-1} + C_x^{-1}]^{-1} \tag{16}$$

The noise propagation on the k^{th} mode will thus be given by the K^{th} diagonal element of P whilst the overall mean square error (excluding under-modelling error) will be given by the trace of matrix P.

If we assume that the errors are uncorrelated and equal such that $V = \sigma^2 I$ and the a priori covariance $C_x \to \infty$ corresponding to no a priori knowledge, we obtain the simple result -

$$P = P_{MAP} = \sigma^2 F^TF \tag{17}$$

A3: PROOF THAT GAVRIELIDES FUNCTIONS ARE THE MINIMUM NORM VECTOR POLYNOMIALS

Consider a set of vector functions $\vec{F}_k(\underline{x})$ obeying -

$$\vec{\nabla} \cdot \vec{F}_k(\underline{x}) = Z_k(\underline{x}) \tag{A1}$$

where $Z_k(\underline{x})$ are the wavefront basis functions (Zernikes)
and which satisfy the boundary condition -

$$\vec{F}_k(\underline{x}) \cdot \vec{dl} = 0 \tag{A2}$$

We have shown in section 3 of this report that the modal coefficients of the wavefront expansion can then be estimated by direct integration as -

$$a_k = -\int_D \vec{F}_k(\underline{x}) \cdot \vec{\nabla}\phi(\underline{x}) d^2x \tag{A3}$$

Consider adding any function $\vec{A}_k(\underline{x})$ to $\vec{F}_k(\underline{x})$ with $\vec{A}_k(\underline{x})$ satisfying the same boundary condition A2 but having zero divergence (i.e. $\vec{\nabla} \cdot \vec{A}_k(\underline{x}) = 0$). It is then clear that the functions $\vec{F}_k(\underline{x})$ are not unique since $\vec{F}_k(\underline{x}) + \vec{A}_k(\underline{x})$ is also a valid solution.

Gavrielides' functions which we will denote as $\vec{G}_k(\underline{x})$ are chosen to be equal to the gradient of an associated scalar function $\xi_k(\underline{x})$. Thus, we have -

$$\vec{G}_k(\underline{x}) = \vec{\nabla}\xi_k(\underline{x}) \tag{A4}$$

Substitution of this relationship into eqs A1 and A2. yields -

$$\nabla^2 \xi_k(\underline{x}) = Z_k(\underline{x}) \tag{A5}$$

$$\vec{\nabla}\xi_k(\underline{x}) \cdot \vec{dl} = 0 \tag{A6}$$

which is Poisson's equation with the corresponding boundary condition. Gavrielides functions are obtained through solution of eq A5 subject to the boundary condition A6.

Consider a set of vector polynomials obeying eqs A1 and A2 given by $\vec{F}_k(\underline{x}) = \vec{G}_k(\underline{x}) + \vec{A}_k(\underline{x})$ where the $\vec{G}_k(\underline{x})$ are Gavrielides functions and $\vec{A}_k(\underline{x})$ are an arbitrary set of functions obeying eqs A1 and A2. It is simple to show that the noise propagation of this set is governed by the vector norm of the functions -

$$\int_D \vec{F}_k(\underline{x}) \cdot \vec{F}_k(\underline{x}) d^2x \tag{A7}$$

The noise propagation due to Gavrielides functions is -

$$N_G = \int_D \vec{G}_k(\underline{x}) \cdot \vec{G}_k(\underline{x}) d^2x \tag{A8}$$

Using eq. A5, standard vector identities and the divergence theorem, this may be expressed as -

$$\int_D \xi_k(\underline{x})\vec{\nabla}^2\xi_k(\underline{x})d^2x + \oint_c \xi_k(\underline{x})\vec{\nabla}\xi_k(\underline{x}) \cdot \vec{dl} \tag{A9}$$

Substitution of eqs A4 and A5 into A9 yield -

$$N_G = \int_D \xi_k(\underline{x})Z_k(\underline{x})d^2x \tag{A10}$$

The noise propagation of the functions $\vec{F}_k(\underline{x})$. may be expressed as -

$$N_F = N_G + N_A + 2\int_D \vec{G}_k(\underline{x}) \cdot \vec{A}_k(\underline{x})d^2x \tag{A11}$$

where N_A is given by -

$$N_A = \int_D \vec{A}_k(\underline{x}) \cdot \vec{A}_k(\underline{x})d^2x \tag{A12}$$

The integral $\int_D \vec{G}_k(\underline{x}) \cdot \vec{A}_k(\underline{x})d^2x$ may be written as -

$$N_A = \int_D \vec{\nabla}\xi_k(\underline{x}) \cdot \vec{A}_k(\underline{x})d^2x \tag{A13}$$

which may in turn be expressed as -

$$N_A = \int_D \vec{\nabla} \cdot (\xi_k(\underline{x})\vec{A}_k(\underline{x}))d^2x - \int_D \xi_k(\underline{x})\vec{\nabla} \cdot \vec{A}_k(\underline{x})d^2x \tag{A14}$$

The second integral in eq. A14 is identically zero since the functions $\vec{A}_k(\underline{x})$ obey $\vec{\nabla} \cdot \vec{A}_k(\underline{x}) = 0$. We may apply the divergence theorem to the first term in eq. A14 -

$$\int_D \vec{\nabla} \cdot (\xi_k(\underline{x})\vec{A}_k(\underline{x}))d^2x = \oint_c \xi_k(\underline{x})\vec{A}_k(\underline{x}) \cdot \vec{dl} \tag{A15}$$

but since the $\vec{A}_k(\underline{x})$ obey the boundary condition $\vec{A}_k(\underline{x}) \cdot \vec{dl} = 0$. the integral $\int_D \vec{G}_k(\underline{x}) \cdot \vec{A}_k(\underline{x})d^2x = 0$ and we have

$$N_F = N_G + N_A \tag{A16}$$

and since N_A is by definition guaranteed to be positive, we have

$$N_F \geq N_G \tag{A17}$$

for arbitrary $\vec{A}_k(\underline{x})$. The Gavrielides functions are thus minimum norm.

Q.E.D.